International Journal of Mechanical, Industrial and Aerospace Sciences
ISSN: 2517-9950
Vol:7, No:12, 2013

A Sliding Mesh Technique and Compressibility Correction Effects of Two-equation Turbulence Models for a Pintle-Perturbed Flow Analysis

J. Y. Heo, H. G. Sung

***Abstract*—**Numerical simulations have been performed for assessment of compressibility correction of two-equation turbulence models suitable for large scale separation flows perturbed by pintle strokes. In order to take into account pintle movement, a sliding mesh method was applied. The chamber pressure, mass flow rate, and thrust have been analyzed, and the response lag and sensitivity at the chamber and nozzle were estimated for a movable pintle. The nozzle performance for pintle reciprocating as its insertion and extraction processes, were analyzed to better understand the dynamic performance of the pintle nozzle.

***Keywords*—**Pintle, sliding mesh, turbulent model, compressibility correction.

I. Introduction

COMBINATION of different burning rate propellants, fracturing of the wall barrier between grains, and pintle stroke in a nozzle can be employed as a technique to change thrust level during a solid motor operation. The research area of a pintle thruster is a critical technology for precise orbit translation and attitude control. This combined research effort has helped to advance aerospace technology. Coon and Yasuhara theoretically computed chamber pressure and thrust as they were affected by the change of the nozzle throat area, and conducted experiments [1]. They, however, were unable to achieve the desired results due to the damage sustained by the pintle component. Dumortier conducted research into minimizing perturbation between the combustion chamber and thrust with a cone shape pintle by using a numerical analysis [2]. Lafond investigated developed a pintle nozzle for the lateral jet of a missile and applied bore to the pintle to reduce the driving load [3]. Wang et al. conducted an Arbitray Lagrangian-Eulerian (ALE) unsteady numerical analysis on a pintle rocket motor in order to research rocket motor thrust control dynamic characteristics considering pintle velocity and the change of the nozzle's inner volume by using dynamic mesh [4]. Experiments on pintle shape and movement, as well as numerical analyses on the effects of pintle shape on nozzle performance, were conducted [5], [6]. Sudden movements of a pintle located inside of a combustion chamber induced a rapid change in the flow field, pressure vibration and transition of combustion phenomena [7]-[9]. Complicated shock waves and flow separation were observed in nozzle, and this shock waves and flow separation were affected by the location of pintle [10].

J. Y. Heo and H. G. Sung are with the Korea Aerospace University, Goyang, Republic of Korea (e-mail: hgsung@ kau.ac.kr).

The shock wave and flow separation induces an interference phenomenon, turbulence in the boundary layer and flow instability [11]. Precisely capturing the shock wave and flow separation is an important factor because flow structure depends on pintle location, and it accompanies flow separation. The interaction of a shock wave and a turbulent boundary layer significantly influences the entire flow field, especially when the shock is strong enough to separate the boundary layer [12]. Therefore, a numerical model with the compressibility effect is required in the supersonic and transitional regions. From this perspective, the object of this research is studying two-equation turbulent model with compressibility correction effects and conformal moving grid technique to achieve more precise numerical results in the pintle-perturbed nozzle flow.

In this study, numerical simulations have been performed for assessment of compressibility correction of two-equation turbulence models suitable for large scale separation flows perturbed by pintle strokes. The two-equation turbulence models, the low Reynolds k-ε and the k-ω SST models with or without compressibility correction proposed by Wilcox and Sarkar are evaluated.

II. Numerical Method

A. Governing Equation

The Favre-averaged governing equations based on the conservation of mass, momentum, and energy for a compressible flow can be written as:

$$\frac{\partial \bar{\rho}}{\partial t}+\frac{\partial \bar{\rho}\tilde{u}_j}{\partial x_j}=0 \tag{1}$$

$$\frac{\partial \bar{\rho}\tilde{u}_i}{\partial t}+\frac{\partial\left(\bar{\rho}\tilde{u}_i\tilde{u}_j+\bar{p}\delta_{ij}\right)}{\partial x_j}=\frac{\partial\left(\bar{\tau}_{ij}-\overline{\rho u_j'' u_i''}\right)}{\partial x_j} \tag{2}$$

$$\frac{\partial \bar{\rho}\tilde{E}}{\partial t}+\frac{\partial\left(\left(\bar{\rho}\tilde{E}+\bar{p}\right)\tilde{u}_j\right)}{\partial x_j}=\frac{\partial\left(\tilde{u}_i\bar{\tau}_{ij}-\overline{\rho h'' u_i''}\right)}{\partial x_j}-\frac{\partial \bar{q}_j}{\partial x_j} \tag{3}$$

B. Turbulence Model and Compressibility Correction

The turbulence models considered for this study are two-equation turbulence models, such as low-Reynolds number k-ε model [13] and k-ω SST model [14].

Inspection of the turbulence kinetic energy equation also

indicates that the Favre-averaged dissipation rate is given by

$$\bar{\rho}\varepsilon = t_{ji}\overline{\frac{\partial u_i''}{\partial x_j}} = \bar{\rho}\varepsilon_s + \bar{\rho}\varepsilon_d \tag{4}$$

where

$$\bar{\rho}\varepsilon_s = \bar{\nu}\overline{\rho\,\omega_i''\omega_i''} \qquad and \qquad \bar{\rho}\varepsilon_d = \frac{4}{3}\bar{\nu}\overline{\rho u_{i,i}'' u_{i,i}''} \tag{5}$$

Based on observations from some older Direct Numerical Simulation (DNS), Sarkar et al. and Zeman postulate that the dilatation dissipation should be a function of turbulence Mach number, M_t, defined by

$$M_t^{\,2} = 2k / a^2 \tag{6}$$

where a is the speed of sound. They further argue that the k and ε equations should be replaced by

$$\frac{\partial \bar{\rho}k}{\partial t} + \frac{\partial\left(\bar{\rho}\tilde{u}_j k\right)}{\partial x_j} = -\bar{\rho}\left(\varepsilon_s + \varepsilon_d\right) + \cdots \tag{7}$$

$$\frac{\partial \bar{\rho}\tilde{\varepsilon}_s}{\partial t} + \frac{\partial\left(\bar{\rho}\tilde{u}_j \tilde{\varepsilon}_s\right)}{\partial x_j} = -C_{\varepsilon 2}\rho\varepsilon_s^{\,2}/k + \cdots \tag{8}$$

where $C_{\varepsilon 2}$ is a closure coefficient. Only the dissipation terms are shown explicitly in (7) and (8) since no changes occur in any other terms. Sarkar and Zeman postulate that the equation for ε_s is unaffected by compressibility. The dilatation dissipation is further assumed to be proportional to ε_s so that they say

$$\varepsilon_d = \xi^* F\left(M_t\right)\varepsilon_s \tag{9}$$

where ξ^* is a closure coefficient and $F\left(M_t\right)$ is a prescribed function of M_t. Building upon the Sarkar formulation and dimensional analysis, Wilcox has postulated a similar model that enjoys an important advantage for wall-bounded flows. The Sarkar and Wilcox formulations differ in the value of ξ^* and the functional form of $F\left(M_t\right)$. The values of ξ^* and $F\left(M_t\right)$ for the Sarkar [15] and Wilcox [16] models are;

Sarkar's Model

$$\xi^* = 1.0, \qquad F\left(M_t\right) = M_t^{\,2} \tag{10}$$

Wilcox's Model

$$\xi^* = 3/2, \quad M_{t_o} = 0.25$$
$$F\left(M_t\right) = \left[M_t^{\,2} - M_{t_0}^{\,2}\right]H(M_t - M_{t_0}) \tag{11}$$

where $H\left(x\right)$ is the Heaviside step function.

C. Numerical Scheme

The conservation equations for moderate and high Mach number flows are well coupled, and the standard numerical techniques perform adequately. In regions of low Mach number flows, however, the energy and momentum equations are practically decoupled and the system of conservation equations becomes stiff. Over in the entire pintle thruster, the flow fields are governed by a wide variety of time scales, from stagnation in the chamber to supersonic flow in the exhaust jet. Such a wide range of time scales causes an unacceptable convergence problem. To overcome the problem, a dual time-integration procedure designed for all Mach number flows is applied. First, a rescaled pressure term is used in the momentum equation to circumvent the singular behavior of pressure at low Mach numbers. Second, a dual time-stepping integration procedure is established. The pseudo-time derivative may be chosen to optimize the convergence of the inner iterations through the use of an appropriate preconditioning matrix that is tuned to rescale the eigenvalues to render the same order of magnitude to maximize convergence. To unify the conserved flux variables, a pseudo-time derivative of the form $\Gamma\partial Z/\partial\tau$ can be added to the conservation equation. Since the pseudo-time derivative term disappears as the solution is converged, a certain amount of liberty can be taken in choosing the variable Z. We take advantage of this by introducing a pressure p' as the pseudo-time derivative term in the continuity equation.

Dual time stepping and LU-SGS are applied for time integration, and the control volume method is used to integrate inviscid fluxes represented by AUSMPW+ and MUSCL and viscous fluxes by central difference. The code is paralleled using an MPI library to speed up the calculation.

III. Model Description

A nozzle was designed for isentropically expanded flow at Mach 2.94, corresponding to a Reynolds number of $1.4\text{x}10^5$ at the exit plane. This study employed the cold flow test model, for which experimental and previous research data are available. The schematics of pintle nozzle and boundary conditions are shown in Fig. 1.

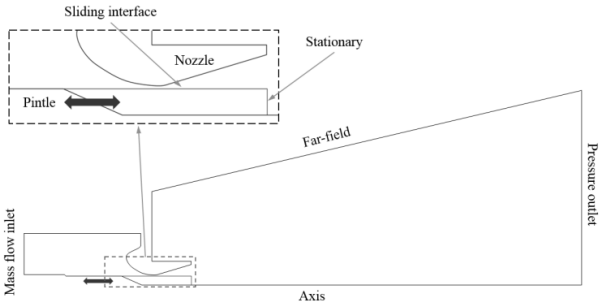

Fig. 1 Schematics of pintle nozzle and boundary conditions

There were approximately 50~52K total grid points, and the

first cell height along the inside of the nozzle is approximately $y^+ = 2$, imposing about five cells in the boundary layer. Several boundary conditions are applied for this study; the mass flow rate for the inlet boundary condition of the chamber, constant pressure outflow boundary conditions for subsonic flow, but switched to extrapolation for the supersonic flow, and no-slip and adiabatic wall boundary condition on the nozzle and pintle walls. In order to investigate the pintle movement effects, a sliding mesh method has been applied.

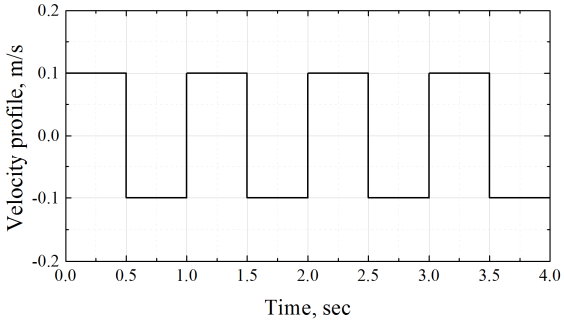

Fig. 2 Pintle velocity profile for each sequence

The pintle operation sequence is shown in Fig. 2. The pintle moves toward the nozzle throat and it instantly turns back to the original location.

IV. Results and Discussion

A. Sliding Mesh

A conformal sliding mesh technique has been applied to investigate the movement effect of a pintle, possessing unsteady flow separation in a pintle nozzle. Fig. 3 represents a moving mesh mechanism on sliding interface for the pintle nozzle. The conformal sliding mesh technique proposed in the study eliminates the flow discontinuity at the moving mesh boundary.

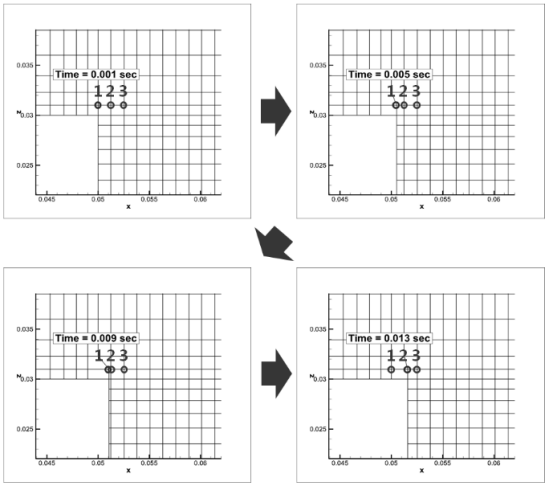

Fig. 3 Moving mesh mechanism for a pintle nozzle

B. Validation

The numerical analysis is implemented under the same condition as the experiment [5]. The numerical results are compared with experimental data conveying the complex flow structure formed as a result of complex shock waves and flow separation in the pintle nozzle.

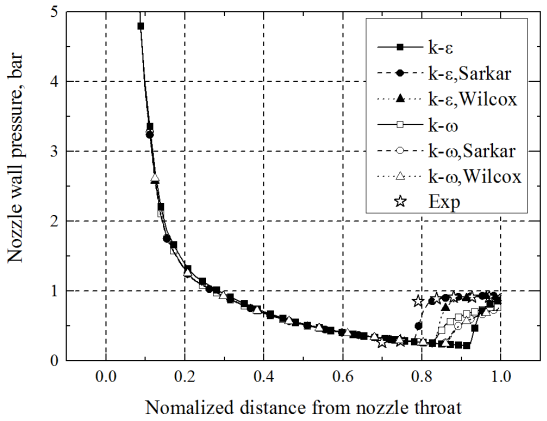

Fig. 4 Pressure distribution along the nozzle wall, model 3

Fig. 4 shows the pressure distribution along the nozzle wall in response to the pintle stroke. At the pintle stroke 0.8, the decaying wall pressure abruptly increases up to the atmospheric pressure at the location 0.77 due to the flow separation which reasonably comparable with the experimental data. As a result, the Sarkar's compressibility correction on Low Reynolds k-ε turbulence model has best predicted the flow separation point and pressure recovery after flow separation on the nozzle wall.

C. Turbulence Model and Compressibility Correction Effects

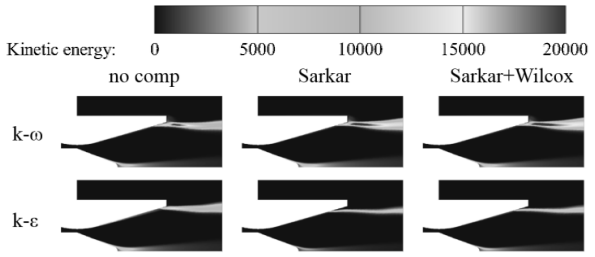

Fig. 5 Kinetic turbulent energy contours in a pintle perturbed nozzle

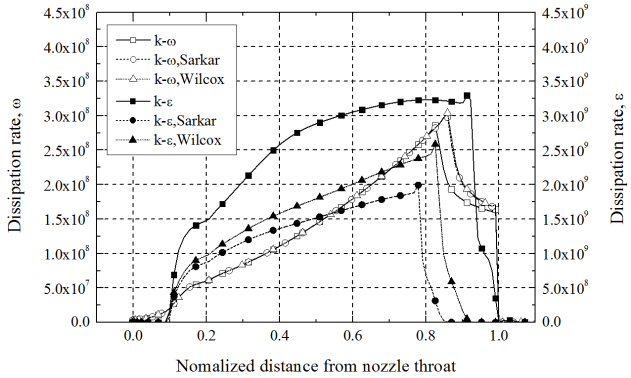

Fig. 6 Dissipation rate distribution along the nozzle wall

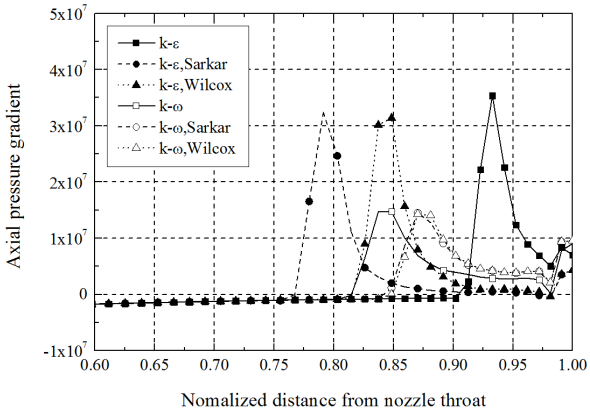

Fig. 7 X-directional pressure gradient along the nozzle wall

The Mach disk location and pressure recovery profiles in flow separation region are noticeably distinct between turbulent models of k-ε and k-ω SST. As shown in Figs. 5-7, kinetic turbulent energy, dissipation rate of turbulent energy, and pressure gradient in the nozzle are analyzed to evaluate turbulent models with or without compression correction

D.Dynamic Characteristics

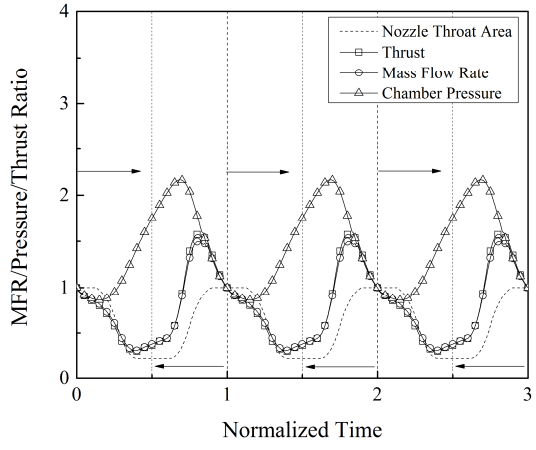

Fig. 8 Comparison of mass flow rate, chamber pressure and thrust

Fig. 8 shows the time history of chamber pressure, thrust, and mass flow rate of the pintle reciprocating to the nozzle throat. The chamber pressure increases as the pintle inserts to the nozzle throat because the nozzle throat area decreases. As the pintle extracted which means the nozzle throat area increases, the chamber pressure does not decreases immediately but it still increases for about 0.22 normalized time because of the time lag of the traveling wave. As the same manner, the chamber pressure does not increase at the moment of the insertion of the pintle as shown in Fig. 8.

The thrust response to the pintle movement shows different tendency to the pressure response. It decreases at the beginning period of the pintle insertion even though the chamber pressure increases and then starts to increase slowly for a while and then move steeply increases. The thrust change can be explained by the explicit relation of pressure and nozzle throat area as following;

$$F \propto P_c A_t \tag{12}$$

where thrust F, chamber pressure P_c and nozzle throat area A_t are represented respectively.

As shown in Fig. 8, the thrust decreases for the nozzle throat area more steeply decreases than the increase of pressure and increases slowly for constant nozzle throat are but the increase of pressure. And then it increases steeply for increase period of both throat area and pressure and decrease because the pressure decreases with no change of throat area. It is note that the prediction of thrust should be conducted through the precise evaluation of chamber pressure and nozzle throat area for the pintle movement.

The mass flow rate $\dot{m}$ has the similar change as the thrust because of the relation of chamber pressure and nozzle throat area as following;

$$\dot{m} \propto P_c A_t \tag{13}$$

The phase difference between pressure and mass flow rate occurs due to the time spent by the wave reflected from the chamber to the nozzle throat.

V. Conclusion

A numerical simulation has been performed to investigate the pintle nozzle characteristics. Unsteady numerical simulation using the sliding mesh scheme has been conducted to observe the dynamic characteristics of the pintle nozzle performance as the pintle moves. The Sarkar's compressibility correction on Low Reynolds k-ε turbulence model has best predicted the flow separation point and pressure recovery after flow separation on the nozzle wall. Within the period of the reciprocating motion of the pintle, the pressure increases up to 2.5 times of the initial pressure, and the thrust varies 50~200% of the initial thrust. As the reciprocal motion of the pintle, the chamber pressure and thrust have phase lag to the pintle movement due to the time difference between the wave

reflected from the nozzle throat to the chamber and the wave from the nozzle throat to the nozzle exit. The hysteresis of thrust and pressure has been observed to the insertion and extraction of the pintle.

REFERENCES

[1] Coon, J. and Yasuhara, W., "Solid Propulsion Approaches for Terminal Steering," AIAA SDIO Interceptor Technology Conference, AIAA 93-2641, 1993.
[2] Dumortier, A., "Hot-gas Valve Development using a Simple Numeric Code," 30th AIAA/ASME/SAE/ASEE Joint Propulsion Conference, AIAA 94-3158, 1994.
[3] Lafond, A. "Numerical Simulation of the Flowfield inside a Hot Gas Valve," 37th Aerospace Sciences Meeting & Exhibit, AIAA 99-1087, 1999.
[4] Li, J., Wang, Z., Zheng, K., Li, J., "Numerical Analysis on Dynamic Response Characteristics of Pintle-controlled Solid Rocket Motor," Journal of Solid Rocket Technology, Vol. 32, No. 1, 2009, pp. 48-52.
[5] Kim, J., "Study on the Effects of Pintle Shapes and Position in Nozzle Flowfield, and Thrust in a Solid Rocket Motor with Pintle Nozzle," Ph.D. Dissertation, Dept. of Mechanical Design Engineering, Chungnam National University, South Korea, 2011.
[6] Kim, J., Park, J., "Investigation of Pintle Shape Effect on the Nozzle Performance," Journal of the Korean Society for Aeronautical & Space Sciences, Vol. 36, No. 8, 2008, pp. 790-796.
[7] Lee, J., "A Study on the Static and Dynamic Characteristics of Pintle-Perturbed Conical Nozzle Flows," Ph.D. Dissertation, Dept. of Mechanical Engineering, Yonsei University, South Korea, 2012.
[8] Park, H., Kim, L., Heo, J., Sung, H., Yang, J., "Numerical Study on Dynamic Characteristics of Pintle Nozzle for Variant Thrust: Part 1," The Korean Society of Propulsion Engineers Spring Conference, 2011.
[9] Heo, J., Kim, K., Sung, H., Yang, J., "Numerical Study on Dynamic Characteristics of Pintle Nozzle for Variant Thrust: Part 2," The Korean Society of Propulsion Engineers Spring Conference, 2012.
[10] Heo, J., Jeong, K., Sung, H., "Numerical Study on Dynamic Characteristics of Pintle Nozzle for Variant Thrust: Part 3," The Korean Society of Propulsion Engineers Spring Conference, 2013.
[11] Johnson, A. D., Papamoschou, D., "Instability of Shock-induced Nozzle Flow Separation," Physics of Fluids, Vol. 22, 2010.
[12] Pearcey, H. H., "Some Effect of Shock-induced Separation of Turbulent Boundary Layers in Transonic Flow Past Aerofoils," Aeronautical Research Council, ARC R&M-3108, 1955.
[13] Yang, Z., and Shih, T. H., "New Time Scale Based Model for Near-Wall Turbulence", AIAA Journal, Vol. 31, No. 7, 1993, pp. 1191-1197.
[14] Menter, F. R., "Two-Equation Eddy-Viscosity Turbulence Models for Engineering Application", AIAA Journal, Vol. 32, No. 8, 1993, pp. 1598-1605.
[15] Sarkar, S., Erlebacher, B., Hussaini, M., and Kreiss, H., "The A-nalysis and Modeling of Dilational Terms in compressible Turbulence", Journal of Fluid Mechanics, 227, 1991, pp. 473-493.
[16] Wilcox, D. C., Turbulence Modeling for CFD, Second Ed. DCW Industries, 2002.